Electronic Supplementary Material (ESI) for Journal of Materials Chemistry B.

Electronic Supplemental Information (ESI)

Fetuin-A Adsorption and Stabilization of Calcium Carbonate Nanoparticles in a Simulated Body Fluid

*Erick S. Vasquez[a], Janice L. Cunningham[b], Justin B. McMahan[b], C. LaShan Simpson[b], and Keisha B. Walters[a]**

[a]Dave C. Swalm School of Chemical Engineering, Mailstop 9595, 330 Swalm Chemical Eng. Bldg., Mississippi State, MS, 39762, USA

[b]Agricultural and Biological Engineering Department, Mailstop 9632, 130 Creelman St., Mississippi State, MS, 39762, USA

*E-mail: kwalters@che.msstate.edu

Keywords: Fetuin-A, $CaCO_3$, calcium carbonate, aggregates, nanoparticles

ESI-1. Infrared spectroscopic analysis of $CaCO_3$ nanoparticles and Fetuin-A

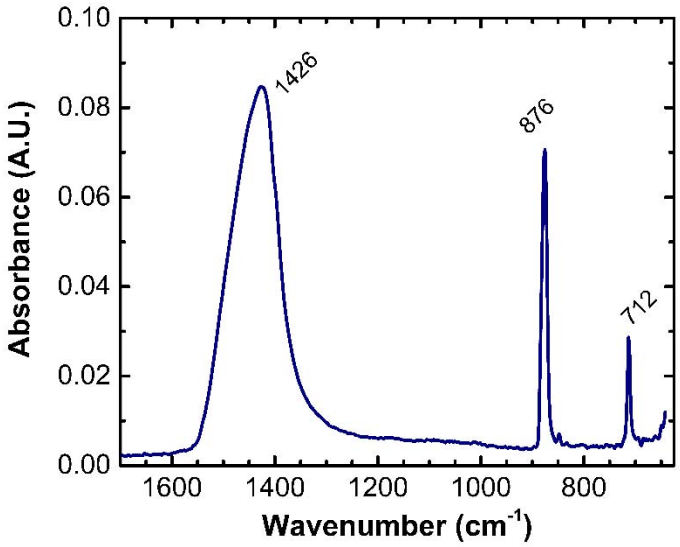

Figure S1. ATR-FTIR spectrum for "as-received" $CaCO_3$ nanoparticles

The infrared adsorption bands for $CaCO_3$ nanoparticles, collected with a DTGS detector and shown in Fig. S1, revealed three distinctive peaks. The CO_3 asymmetric vibration at 1426 cm^{-1} (ν_3), asymmetric vibration 876 cm^{-1} (ν_2), and symmetric vibration at 712 cm^{-1} (ν_4) are used to confirm the crystalline state of the sample. With these peaks, the $CaCO_3$ nanoparticles used in this study are assigned to a calcite crystalline form.[1-3] A brief discussion on the infrared absorption bands and peak identification for Fetuin-A glycoprotein are displayed in Figure S2, and summarized in Table S1. A very strong/broad band was observed near ~3300 cm^{-1}, corresponding to the primary amine symmetric/asymmetric stretch vibrations. This absorption band, present in the Fetuin-A spectrum as shown in Figure S2, have been previously assigned to other glycoproteins, and could also be part of O–H stretching vibrations from amino acid structures.[4] Additionally, methylene absorption bands were also observed. Specifically, $-CH_2$ asymmetric and symmetric stretching bands are reported at 2960 and 2935 cm^{-1}, respectively. A symmetric C-H stretching band for –

CH_3 was observed at 2875 cm^{-1}. Additional methylene absorption bands, in the fingerprint region, were also present at 1453 cm^{-1}, 1379 cm^{-1}, and 860 cm^{-1} wavenumbers, with detailed functional group identification presented in Table S1.

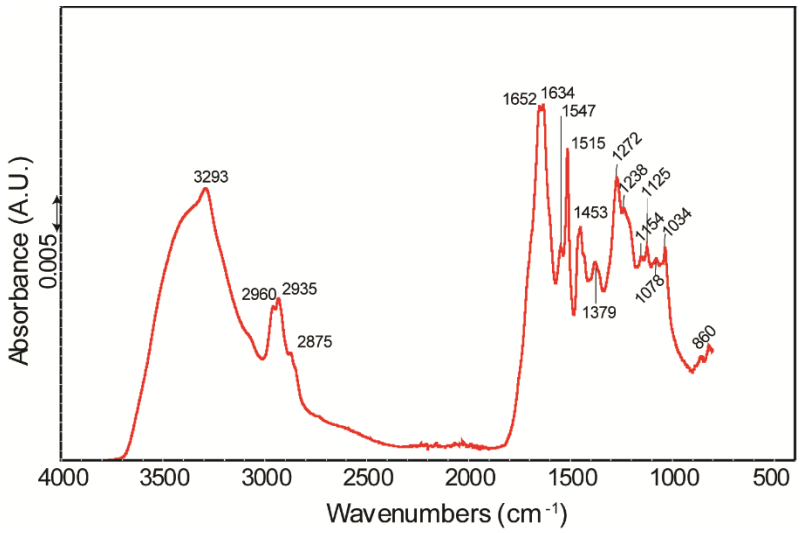

Figure S2. ATR-FTIR spectrum for Fetuin-A with primary peaks identified.

The specific infrared regions for the analysis of proteins are the amide I, II, and III absorption bands.[5, 6] For amide I, Fetuin-A showed a peak at 1652 cm^{-1}, primarily due to C=O stretching vibrations, that are useful in determining the secondary structure of the protein backbone. As discussed in Section 2.1, the deconvolution of this region showed the presence of secondary structures, such as β-sheet and α-helix. An amide-II peak for Fetuin-A was observed at 1547 cm^{-1}, which is attributed primarily to N–H deformations; however, it also depends on C–N and C–C stretching vibrations, and C–O in plane-bending.[6] This region was also deconvoluted and analyzed before and after adsorption of Fetuin-A on CaCO3 nanoparticle aggregates (Section 2.1). One of these absorptions, the C–O in plane-bending, was observed for the Fetuin-A infrared spectrum at

1515 cm^{-1} wavenumber (Table S1). Lastly, an amide III peak was present at 1238 cm^{-1}, and corresponds primarily to N–H bending and C–N stretching vibrations.

The O–H absorption deformation bands for Fetuin-A were observed for primary (1272 cm^{-1}), secondary (1125 cm^{-1}), and tertiary (1153 cm^{-1}) alcohols, attributed to the presence of multiple amino acid residues in Fetuin-A.[7, 8] The presence of multiple amino acids is further confirmed by absorbances for primary (1078 cm^{-1}) and secondary (1054 cm^{-1}) α-carbon (C–N) groups and for the H-C(COOH) out-of-plane bending deformation band at 860 cm^{-1}, which are characteristic of amino acids.

Table S1. IR band assignments for Fetuin-A and Fetuin-A/$CaCO_3$ complexes.[a]

Absorption Band (cm^{-1})	Origin	Assignment
≈ 3400 - 3300	N–H / O–H	Primary amine, symmetric and/or asymmetric region. O–H stretching vibrations
2960	C–H	$–CH_2$ asymmetric stretch
2935	C–H	$–CH_2$ symmetric stretch
2875	C–H	$–CH_3$ symmetric stretch
1652	C=O	Amide I band, carbonyl stretch
1634	N–H	Primary amine, deformation
1547	N–H	Amide II band, N–H deformation
1515	C–O	Amino acid chain absorption, tyrosine, tyr–OH
1453	C–H	$–CH_2$ deformation, symmetric stretch, $–CH_3$ asymmetrical bending vibration.
1379	C–H	$–CH_3$ symmetric in-plane bending vibration
1272	C–O	–CO stretch, carboxylic acids or primary alcohols
1238	N–H	Amide III band, secondary amine
1153	O–H	Saturated tertiary alcohol, deformation
1125	O–H	Saturated secondary alcohol, deformation
1078	C–N	Primary amine, stretch, primary α-carbon of amino acids
1034	C–N	Primary amine, stretch, secondary α-carbon of amino acids
860	C–H	H-C(COOH), out-of-plane bending deformation

[a] Group frequency wavenumbers were obtained from selected references.[4, 6, 9-12]

Figure S3 shows the high-resolution XPS scans for nitrogen on $CaCO_3$ nanoparticles (Figure S3A) and Fetuin-A/$CaCO_3$ complexes (Figure S3B).

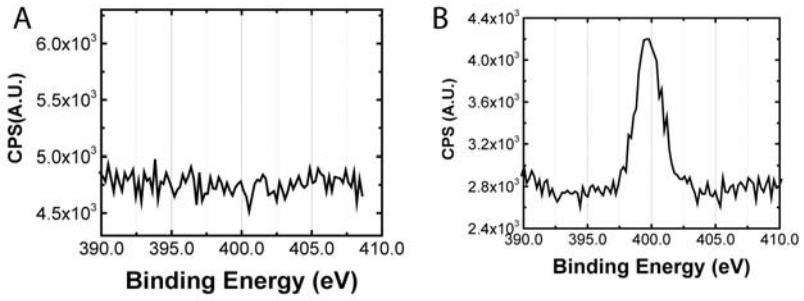

Figure S3. Nitrogen high-resolution XPS scans for $CaCO_3$ nanoparticles (A) and Fetuin-A/$CaCO_3$ complexes (B) demonstrate the presence of nitrogen, a characteristic element present in Fetuin-A and many other proteins, confirming the adsorption of Fetuin-A onto $CaCO_3$ particles.

ESI-2. Time-dependent study of Fetuin-A/$CaCO_3$ complexes

To further confirm the stability of the Fetuin-A/$CaCO_3$ complexes, a 10 μM Fetuin-A solution, which has been shown to be sufficient for the stabilization of calciprotein particles for up to 24 h,[13] was combined with an $CaCO_3$ aqueous solution. Over a two-month period, an aqueous solution of Fetuin-A/$CaCO_3$, with a mass ratio of 5.9, was studied for changes in particle size. DLS measurements were conducted, and a summary of the measured effective diameters is shown in Figure S4A. At 3 h after Fetuin-A/$CaCO_3$ complexation, an initial stabilization period was observed that showed a slightly larger particle size distribution, but no significant difference in particle size. This sample was left at room temperature (~22 °C) for one month, and again characterized with DLS characterization, an ~29% increase in effective diameter was observed (Figure S4A). After a two-month incubation period, the effective diameter of the complexed Fetuin-A/$CaCO_3$ had increased to 1070 nm effective diameter, approximately 200% larger than

the average diameter measured at 3 h. By examining the diameter by number, a better comparison of changes in the size of the Fetuin-A/$CaCO_3$ complexes can be made, as large-size agglomerates can be eliminated from the calculation of average diameter. For instance, after a one-month incubation time a decrease in 24 % diameter by number was observed. After a two-month period, a total of 60% decrease in diameter by number was achieved. To further examine the particle morphologies associated with these DLS data, TEM images were collected *in-situ* to avoid artificial particle aggregation due to drying. Figure S4B, corresponding to the 2 month sample, shows a small particles (~110 nm); however, other smaller particles were also observed, possibly due to decomposition of $CaCO_3$ nanoparticle aggregates. This small/non-homogeneous $CaCO_3$ nanoparticle aggregates will indeed have an effect on the effective diameter of the Fetuin-A/$CaCO_3$ complexes, corresponding to the high effective diameter values reported in Figure S4A. Thus, a report using diameter by number will be more efficient for this type of mineralo-protein complexes in water.

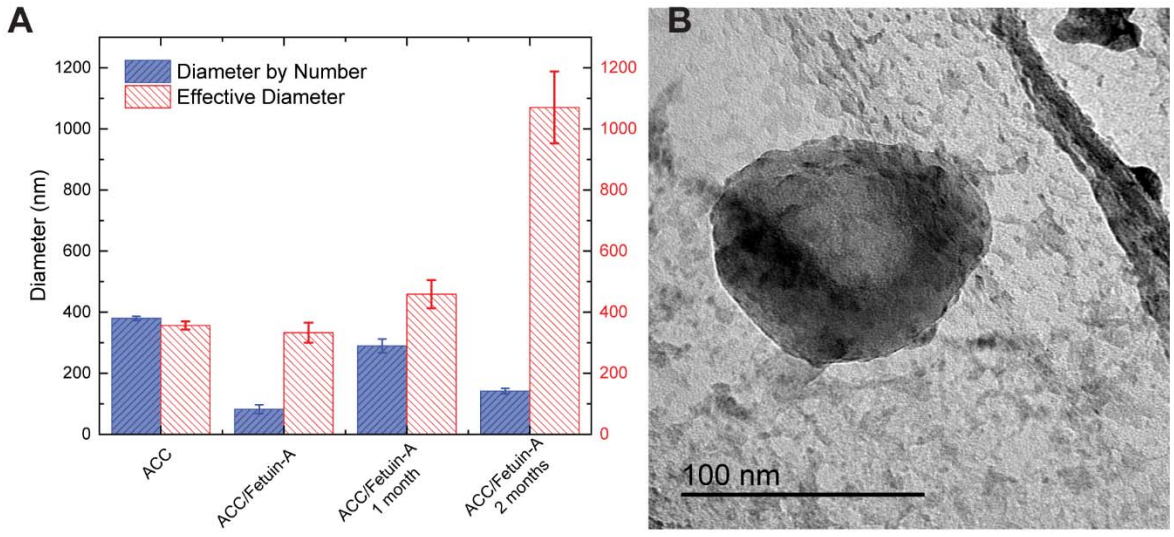

Figure S4. (A) A larger distribution of effective hydrodynamic diameter was measured for Fetuin-A/$CaCO_3$ complex, in comparison to the $CaCO_3$ nanoparticle in solution, after a 3-hour period. At one and two months of incubation at ambient conditions, the average particle effective diameter had increased by 29% and 200%, respectively. Conversely, particle diameter by number decreased after two months by a total of 60 %. (B) Cryo TEM of Fetuin-A/$CaCO_3$ incubated for two months,

reveals a small particle (core) surrounded by large aggregates (shell) with decomposed $CaCO_3$ nanoparticles with similar size to the diameter by number obtained with DLS.

Morphological characterization of the Fetuin-A/$CaCO_3$ complexes was further examined with *in-situ* TEM as shown in Figure S5. Results show similar spherical aggregates due to the formation of Fetuin-A/$CaCO_3$ complexes (Fig. S5A), and other smaller particles. The non-homogenous particles observed in Figure S5(B,C) are attributed to the decomposition of the Fetuin-A/$CaCO_3$ complexes, resulting in the formation of soluble nanoparticles.

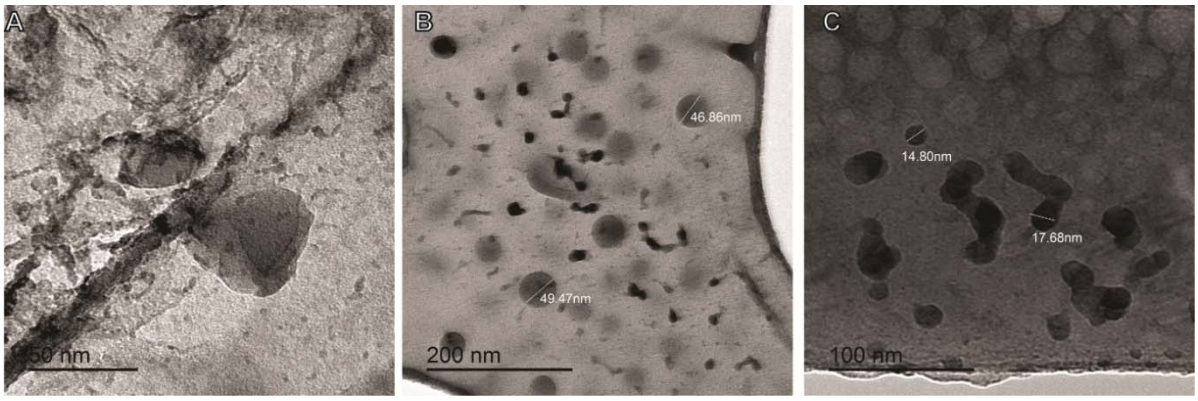

Figure S5. Morphological changes after two-months were examined with cryo TEM images showing A) aggregates with small spheres ~ 50 nm diameter, B) small darker areas possibly caused by the presence of dissolved $CaCO_3$ nanoparticles, and C) elongated structures.

ESI-3. UV-Vis Absorbance of Fetuin-A, $CaCO_3$ particles, and Fetuin-A/$CaCO_3$ complexes.

Fetuin-A adsorption on $CaCO_3$ particles was demonstrated by an initial increase in effective diameter, followed by a decrease in particle size as characterized by using diameter by number via DLS measurements. UV-Vis measurements (Figure S6) were conducted immediately after addition of Fetuin-A to $CaCO_3$ particles in order to demonstrate any particle molecular absorption shift. Results show a slight molecular absorbance peak-shift in the region of 270-280 nm as Fetuin-A/$CaCO_3$ complexes are formed in water. This result is possibly due to the particular interactions between the secondary structures of the Fetuin-A neat protein, as it starts to form a complex

structure with $CaCO_3$ particles. In addition, this peculiar shift suggest the possible mechanism discussed with IR analysis on secondary protein structure binding mechanisms.

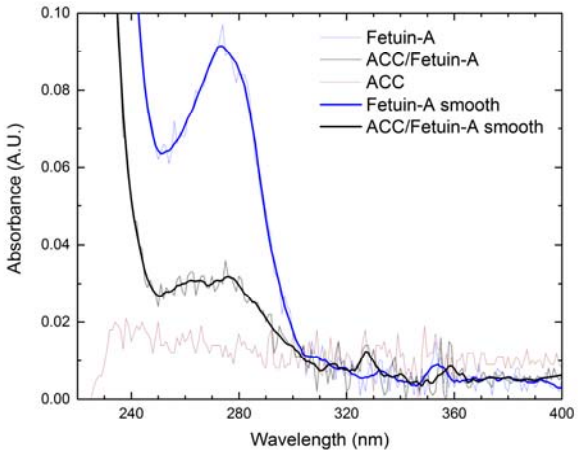

Figure S6. UV-Vis spectra for Fetuin-A, $CaCO_3$, and Fetuin-A/$CaCO_3$ complexes.

References

1. E. Foran, S. Weiner and M. Fine, *Sci. Rep.*, 2013, **3**.
2. J. D. Rodriguez-Blanco, S. Shaw and L. G. Benning, *Nanoscale*, 2011, **3**, 265-271.
3. M. A. Legodi, D. de Waal, J. H. Potgieter and S. S. Potgieter, *Minerals Engineering*, 2001, **14**, 1107-1111.
4. M. M. Patel, J. D. Smart, T. G. Nevell, R. J. Ewen, P. J. Eaton and J. Tsibouklis, *Biomacromolecules*, 2003, **4**, 1184-1190.
5. P. S. W. Yeung, G. Eskici and P. H. Axelsen, *Biochimica et Biophysica Acta (BBA) - Biomembranes*, 2013, **1828**, 2314-2318.
6. A. Barth, *Biochimica et Biophysica Acta (BBA) - Bioenergetics*, 2007, **1767**, 1073-1101.
7. T. Schinke, C. Amendt, A. Trindl, O. Pöschke, W. Müller-Esterl and W. Jahnen-Dechent, *Journal of Biological Chemistry*, 1996, **271**, 20789-20796.
8. N. Sonveaux, A. B. Shapiro, E. Goormaghtigh, V. Ling and J.-M. Ruysschaert, *Journal of Biological Chemistry*, 1996, **271**, 24617-24624.
9. M. Baldassarre, R. Galeazzi, B. Maggiore, F. Tanfani and A. Scirè, *Biochimie*, 2014, **102**, 19-28.
10. M. Khajehpour, J. L. Dashnau and J. M. Vanderkooi, *Analytical Biochemistry*, 2006, **348**, 40-48.
11. V. r. Kopecký Jr, R. Ettrich, K. Hofbauerová and V. r. Baumruk, *Biochem Bioph Res Co*, 2003, **300**, 41-46.
12. R. M. Silverstein, F. X. Webster and D. J. Kiemle, *Spectrometric identification of organic compounds*, John Wiley & Sons, Hoboken, NJ, 7th edn., 2005.
13. A. Heiss, A. DuChesne, B. Denecke, J. Grötzinger, K. Yamamoto, T. Renneé and W. Jahnen-Dechent, *Journal of Biological Chemistry*, 2003, **278**, 13333-13341.